

## Full Paper

## Synthesis, Biological Evaluation and Molecular Docking of Calix[4]arene-Based $\beta$ -Diketo Derivatives as HIV-1 Integrase Inhibitors

Zaigang Luo<sup>1</sup>, Yu Zhao<sup>1</sup>, Chao Ma<sup>1</sup>, Zhipeng Li<sup>2</sup>, Xuemei Xu<sup>2</sup>, Liming Hu<sup>2</sup>, Nianyu Huang<sup>3</sup>, and Hongqiu He<sup>4</sup>

<sup>1</sup> College of Chemical Engineering, Anhui University of Science & Technology, Huainan, P. R. China

<sup>2</sup> College of Life Sciences and Bioengineering, Beijing University of Technology, Beijing, P. R. China

<sup>3</sup> College of Chemistry and Life Sciences, China Three Gorges University, Yichang, P. R. China

<sup>4</sup> Chongqing Academy of Science and Technology, Chongqing, P. R. China

In this publication, we design and report the synthesis of calix[4]arene-based  $\beta$ -diketo derivatives as novel HIV-1 integrase (IN) inhibitors. The target compounds were obtained using Claisen condensation, and their structures were characterized by NMR and ESI-MS. Preliminary bioassays showed that calix[4]arene-based  $\beta$ -diketo derivatives inhibit strand transfer (ST) with  $IC_{50}$  values between 5.9 and 21.2  $\mu$ M. Docking studies revealed the predominant binding modes that were distinct from the binding modes of raltegravir, which suggests a novel binding region in the IN active site. Moreover, these compounds are predicted not to interact with some of the key amino acids (GLN148 and ASN155) implicated in viral resistance. Therefore, this series of compounds can further be investigated for a possible chemotype to circumvent resistance to clinical HIV-1 IN inhibitors.

**Keywords:** Calix[4]arene /  $\beta$ -Diketo derivatives / HIV-1 integrase inhibitors / Molecular docking / Synthesis

Received: October 22, 2014; Revised: December 30, 2014; Accepted: January 6, 2015

DOI 10.1002/ardp.201400390



Additional supporting information may be found in the online version of this article at the publisher's web-site.

### Introduction

HIV-1 integrase (IN), which inserts a double-stranded DNA copy of the viral RNA genome into the chromosomes of an infected cell through a multi-step process that involves 3'-processing (3'-P) and strand transfer (ST) or integration, is an essential enzyme necessary for the replication of the HIV virus [1]. Since IN has no homologue in human cells, it has been recognized as a promising target that were exemplified by the FDA approved HIV-1 IN inhibitors (raltegravir, elvitegravir, and dolutegravir) and those under advanced clinical trials [2].

Over the last two decades, numerous small-molecule HIV-1 integrase inhibitors have been described, the most predominant class of inhibitors being the diketo acids (DKAs) [3], and the DKA moiety was believed to be the most crucial pharmacophore for the inhibition of IN inhibitors [4]. It is believed that their IN-binding mechanism is connected to the presence of DKA pharmacophoric motif which could be involved in a functional sequestration of one or both divalent metal ions in the enzyme catalytic site to form a ligand- $M^{2+}$ -IN complex. This would subsequently block the transition state of the IN-DNA complex by competing with the target DNA substrate [5]. Raltegravir, elvitegravir, and dolutegravir, optimized from the initial DKA pharmacophore, were believed to inhibit IN function at the strand transfer stage by a similar mechanism [6]. However, the partial cross-resistance with raltegravir and elvitegravir has been already found for this compound [7, 8]. Dolutegravir, a second generation integrase strand transfer inhibitor, displays superior characteristics to raltegravir, but partially shares

**Correspondence:** Dr. Zaigang Luo, College of Chemical Engineering, Anhui University of Science & Technology, Huainan 232001, P. R. China.

**E-mail:** luozi139@163.com

**Fax:** +86-554-6668485

the resistance pathways [9]. Due to the limited chemical space available for designing inhibitors of the catalytic activity of IN inevitable overlap of resistance for second generation integrase strand transfer inhibitors is likely [10]. Thus, it is imperative to design new chemical classes as new generation HIV-1 integrase inhibitors possessing novel mechanism of action that not only have potent inhibitory activities, but also have the potential to circumvent the viral resistance to present IN inhibitors.

As assessed by recent reviews [11, 12], calixarenes have been given special attention as new molecular platform for the design and development of new drugs. Many pharmacological properties are described for calixarenes (such as antiviral, antibacterial, anticancer) [12]. Anti-HIV activity of calixarene derivatives has been initially reported by Hwang *et al.* [11, 12]. Subsequently, calixarene derivatives were described as inhibitors of fusion, integrase, and protease enzyme in HIV infection [11, 12]. Also, few investigations of calixarenes as new chemical entities with distinct anti-HIV activities have been made [13, 14]. However, the mechanism of inhibition of HIV activity of the calixarene derivatives is not clear until now.

Taking into consideration the above facts, we recently used the calix[4]arene skeleton as a platform to design a new class of integrase inhibitors **1a–h** (Fig. 1) [15]. Compounds **1e–h** were active toward IN strand transfer reaction (**1e**: ST,  $IC_{50} = 7.4 \mu\text{M}$ ; **1f**: ST,  $IC_{50} = 8.8 \mu\text{M}$ ; **1g**: ST,  $IC_{50} = 6.1 \mu\text{M}$ ; **1h**: ST,  $IC_{50} = 10.9 \mu\text{M}$ , respectively), while **1a–d** showed no activities. In order to investigate whether the 1,2,3-triazole moieties of **1a–h** play an important role in the ST assay or not, therefore, in the present study, we design and synthesize another series of novel calix[4]arene derivatives **4a–j** (Fig. 1) incorporating two  $\beta$ -diketo subunits disposed in alternate position at the lower rim, which have simplified structures by deleting 1,2,3-triazole moieties compared with **1a–h**, and evaluate their anti-IN

activities against HIV-1. It may be helpful to understand the mechanism of this novel class of IN inhibitors. Furthermore, to gain understanding of the binding mode at the IN active site and provide insights for further structure-based drug design, molecular docking study was performed on the selected molecules, **1g** and **4i**.

## Results and discussion

### Chemistry

Depicted in Scheme 1 is our synthetic route developed to allow for efficient introduction of  $\beta$ -diketo moieties on the calix[4]arene skeleton toward the end of the synthesis. The synthesis of inhibitors **4a–j** starts with treatment of *tert*-butylcalix[4]arene **1a** and calix[4]arene **1b** [16] with ethyl bromoacetate in DMF to obtain the intermediates **2a** and **2b** [17]. Then, compounds **2a** and **2b** underwent Claisen condensation with a range of acetophenones **3a–e** to afford the *tert*-butylcalix[4]arene-based  $\beta$ -diketo derivatives **4a–e** and calix[4]arene-based  $\beta$ -diketo derivatives **4f–j** in the alkaline medium (NaH) with a moderate yield (42–71%).

The new compounds have been characterized by a combination of  $^1\text{H}$  NMR,  $^{13}\text{C}$  NMR, and MS (ESI). The NMR spectra of the title compounds revealed that both the *tert*-butylcalix[4]arene and calix[4]arene moieties maintain the cone conformation [18, 19]. The bridging methylene groups of **4a–j** exhibit two sets of doublets (absorptions of the doublets near  $\delta$  3.5 and 4.3 ppm,  $J = 13.2 \text{ Hz}$  for  $\text{ArCH}_2\text{Ar}$  protons) in their  $^1\text{H}$  NMR spectra. And in the  $^{13}\text{C}$  NMR spectra, the methylene carbon appears as one signal (absorption near 31 ppm for methylene carbon of  $\text{ArCH}_2\text{Ar}$ ). The chemical shift values are close to those reported for other calix[4]arene molecules in the same conformation [20, 21]. Meanwhile, the

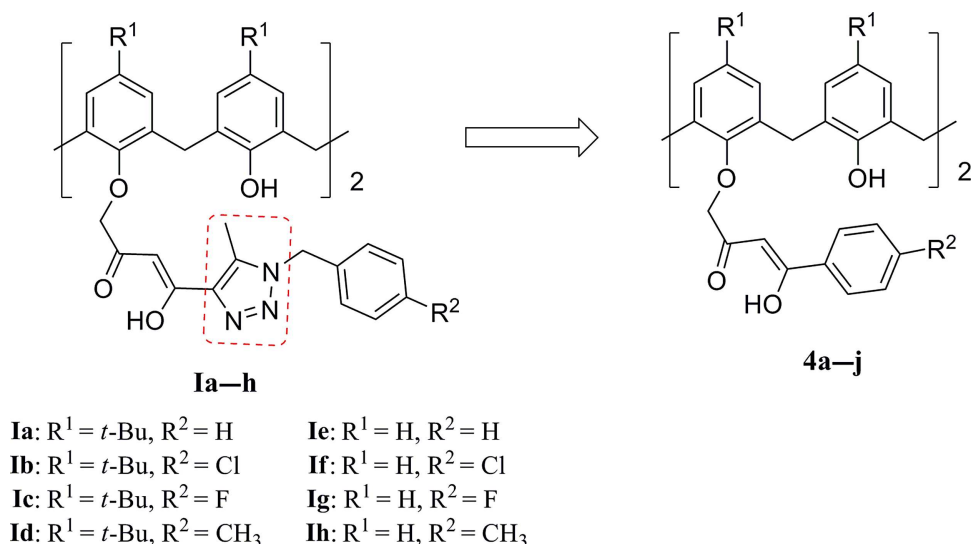
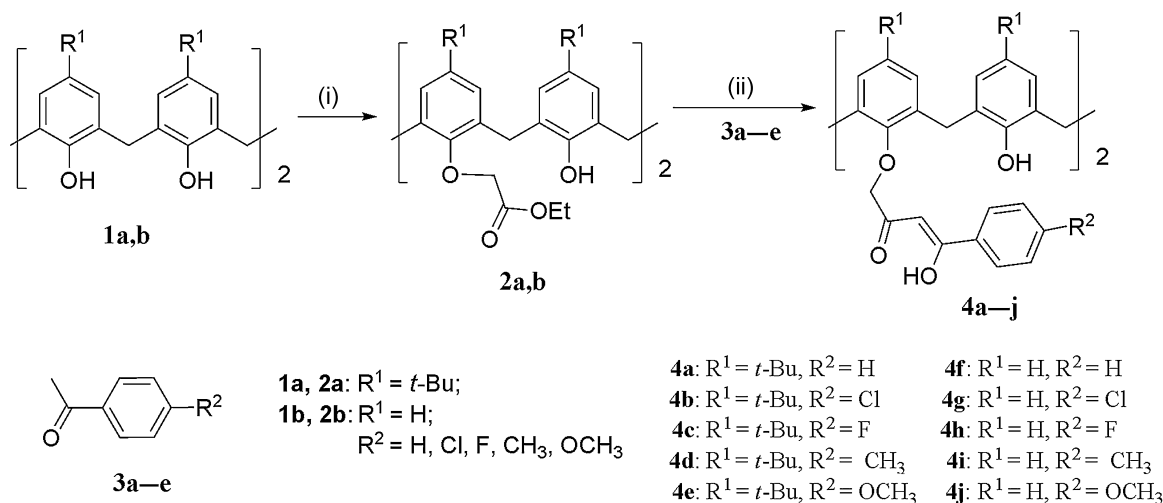


**Figure 1.** Design of novel calix[4]arene-based  $\beta$ -diketo derivatives as IN inhibitors.



**Scheme 1.** Reagents and conditions: (i) BrCH<sub>2</sub>COOEt, K<sub>2</sub>CO<sub>3</sub>, DMF, 60–80°C; (ii) NaH, THF, reflux.

$\beta$ -diketo moiety possess enol-keto tautomerism and the enol configuration is usually the main configuration in the CDCl<sub>3</sub> solvent [22]. From the NMR spectra, the enol configuration of the  $\beta$ -diketo moieties of **4a–j** was also observed in CDCl<sub>3</sub>. This was readily proved by their <sup>1</sup>H NMR (absorption near 7.5 ppm for the methylene proton of the  $\beta$ -diketo moiety) and <sup>13</sup>C NMR spectra (absorption for the methylene carbon of the  $\beta$ -diketo moiety near 97 ppm), respectively.

### Biological evaluation

The inhibition effects of the calix[4]arene derivatives **4a–j** were measured by an HIV-1 integrase strand transfer activity assay, which was carried out as described previously [23]. As shown in Table 1, *p*-*tert*-butylcalix[4]arene derivatives **4a–e** proved to be inactive in the ST assay, but the calix[4]arene derivatives **4f–j** exhibit activities at low micromolar concentrations (ST, IC<sub>50</sub> = 5.9–21.2  $\mu$ M). In comparing the potencies of **4f–j** and **4a–e** in the ST assay, it was seen that removal of the *tert*-butyl groups at the upper rim of calix[4]arene in **4a–e** gave **4f–j** improved IN inhibition activities. The most potent derivative is **4g**, which IC<sub>50</sub> value for strand transfer is 5.9  $\mu$ M. This experimental observation seems to indicate that the bulky *tert*-butyl groups of **4a–e** show reduced combination ability with integrase comparable to H atoms at the upper rim of calix[4]arene, which is similar to the *p*-*tert*-butylcalix[4]arene derivatives **1a–d** in our previous study [15].

Moreover, in order to investigate the substituent effect on the phenyl ring adjacent to  $\beta$ -diketo moiety, electron-donating and electron-withdrawing groups were utilized (**4a–j**). Interestingly, the IC<sub>50</sub> values of **4h** with an electron-withdrawing F atom on the phenyl ring (ST, IC<sub>50</sub> = 13.4  $\mu$ M) and **4i** with an electron-donating CH<sub>3</sub> group on the phenyl ring (ST, IC<sub>50</sub> = 13.1  $\mu$ M) are almost equal to each other. And the similar inhibition activities are also exhibited between **4f** with no substitution on the phenyl ring (ST, IC<sub>50</sub> = 16.3  $\mu$ M)

and **4j** with an electron-donating OCH<sub>3</sub> group on the phenyl ring (ST, IC<sub>50</sub> = 21.2  $\mu$ M). While **4g**, with Cl substitution on the phenyl ring, showed the best anti-IN activities. This observations somewhat indicate that such substitution has no notable impact on their activities. Compared with the slightly different inhibition activities between **1e–h** (ST, IC<sub>50</sub> = 6.1–10.9  $\mu$ M) and **4f–j** (ST, IC<sub>50</sub> = 5.9–21.2  $\mu$ M), the 1,2,3-triazole moieties existing in the skeleton of calix[4]arene derivatives of **1e–h** maybe do not play an important role in the ST assay.

### Molecular docking

In order to explore the binding mode of these compounds against the catalytic active site of IN, a docking study of the

**Table 1.** Inhibition of HIV-1 integrase strand transfer catalytic activities<sup>a)</sup>.

Compounds	R <sup>1</sup>	R <sup>2</sup>	IC <sub>50</sub> ( $\mu$ M) <sup>b)</sup>
<b>4a</b>	<i>t</i> -Bu	H	–c
<b>4b</b>	<i>t</i> -Bu	Cl	–c
<b>4c</b>	<i>t</i> -Bu	F	–c
<b>4d</b>	<i>t</i> -Bu	CH <sub>3</sub>	–c
<b>4e</b>	<i>t</i> -Bu	OCH <sub>3</sub>	–c
<b>4f</b>	H	H	16.3
<b>4g</b>	H	Cl	5.9
<b>4h</b>	H	F	13.4
<b>4i</b>	H	CH <sub>3</sub>	13.1
<b>4j</b>	H	OCH <sub>3</sub>	21.2
Raltegravir			0.86

–c indicates that the HIV-IN inhibitory effect was less than 50% at the initial concentration (50  $\mu$ M).

<sup>a)</sup>HIV-1 IN inhibitory activities were measured according to the procedure described [23].

<sup>b)</sup>Inhibition of strand transfer.

compounds **lg** and **4i** was performed using AutoDock 4.2 software package and the aid of the AutoDock Tools [24]. The X-ray structure of prototypic foamy virus integrase (PFV-IN) with DNA and two  $Mg^{2+}$  ions (PDB: 3OYA) was selected for the docking study since it has been demonstrated that PFV IN is a good model for the development of HIV-1 IN inhibitors [25]. Moreover, the secondary structures of the HIV-1 IN catalytic core domain and PFV IN have a high similarity with calculated root-mean square deviations [25, 26]. Raltegravir was also re-docked into the X-ray structure of 3OYA in order to validate the docking protocol, and the docking results are shown in Figs. 2 and 3.

Fig. 2a, b, and c depict the binding of raltegravir, **lg** and **4i** in the active site, respectively. The docking poses of raltegravir showed a similar binding mode with the X-ray position (Fig. 2a) [25]. The *p*-fluorobenzyl group and the oxadiazole ring of raltegravir were accommodated at the hydrophobic

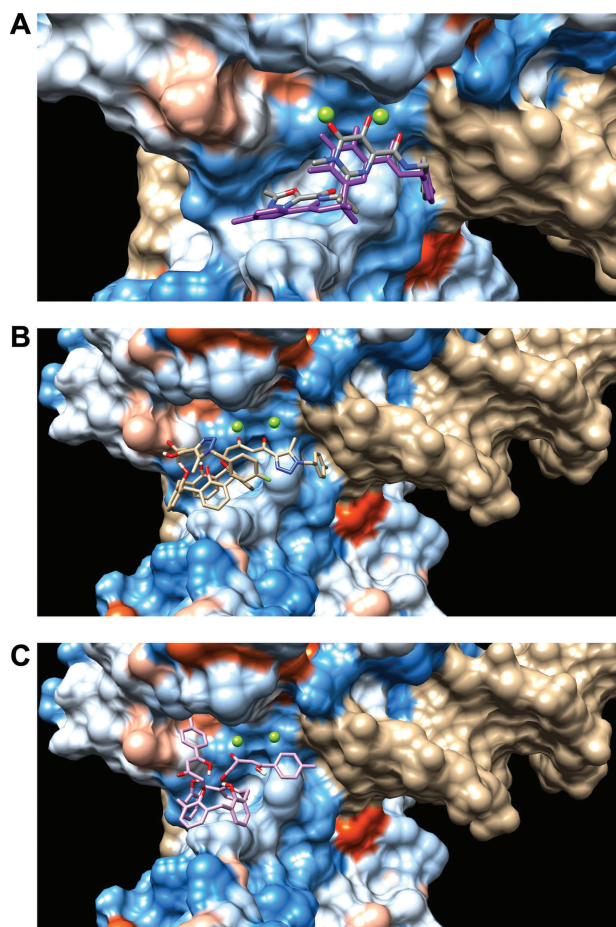


**Figure 2.** The best docking position of raltegravir, **lg** and **4i** in the active site of PFV IN. The green ball represents  $Mg^{2+}$ ; (a) the gray stick represents the docking position of raltegravir; (b) the gold stick represents the docking position of **lg**; (c) the light purple stick represents the docking position of **4i**. Drug atoms are colored: purple and gray, C; blue, N; green, F; red, O.

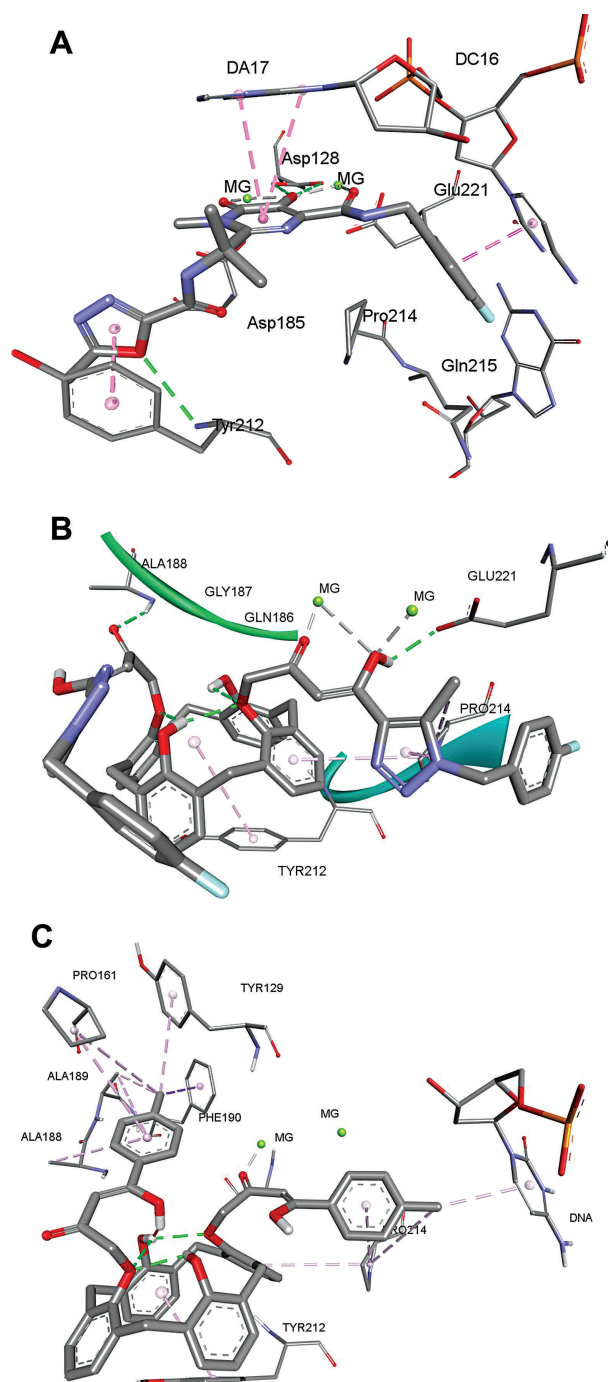


**Figure 3.** Interactions of compounds raltegravir (a), **lg** (b) and **4i** (c) with catalytic residues of PFV IN. Intermolecular and intramolecular hydrogen bond interactions were displayed by green dash line; hydrophobic interactions were displayed by pink dash line; the interactions between magnesium and oxygen of inhibitor were displayed by gray dash line. The green ball represents  $Mg^{2+}$ . Drug atoms are colored: gray, C; blue, N; green, F; red, O.

cavity, and the pyrimidone ring of raltegravir formed metal chelation with the two  $Mg^{2+}$  ions. The macrocyclic skeleton of calix[4]arene of **lg** and **4i** could occupy the hydrophobic cavity of the catalytic core region of IN (Fig. 2a and b). Obviously, one of the triazolyl  $\beta$ -diketo arms of **lg** formed metal chelation with the two  $Mg^{2+}$  ions, but the nitrogen of 1,2,3-triazole moiety did not chelate with the  $Mg^{2+}$  ions. The distortion of the other triazolyl  $\beta$ -diketo arm of **lg** was also observed, thus it was not accommodated at the hydrophobic cavity in the IN active site (Fig. 2b). In Fig. 2c, one of the  $\beta$ -diketo arms of **4i** could dock into the hydrophobic cavity of the catalytic core region of IN, and the other  $\beta$ -diketo arm partially chelated with one of the two  $Mg^{2+}$  ions, for the  $\beta$ -diketo moieties are not at the same side, that is not coplane.

Fig. 3a, b, and c show the binding interactions of raltegravir, **lg** and **4i** with PFV IN. In Fig. 3a, The *p*-fluorobenzyl group of raltegravir interacts with DC16 via  $\pi$ - $\pi$  interaction. And the oxadiazole ring of raltegravir interacts with IN amino acid residue TYR212 via  $\pi$ - $\pi$  interaction and hydrogen bond interaction. The pyrimidone ring of raltegravir plays an important role, which formed metal chelation with the two  $Mg^{2+}$  ions and interacted with DA17 via  $\pi$ - $\pi$  interactions and IN amino acid residue ASP128 via hydrogen bond interactions.

The macrocyclic skeleton of calix[4]arene moiety of **lg** and **4i** may be fit for occupying the hydrophobic cavity and interact with TYR212 and PRO214 via  $\pi$ - $\pi$  interactions. The poor inhibitory activities of compounds **la-d** and **4a-e** probably attribute to the bulky *tert*-butyl groups, which probably prevent the macrocyclic skeleton of *tert*-butylcalix[4]arene moiety from entering into the same hydrophobic cavity region.

In Fig. 3b, the oxygen of the distorted triazolyl  $\beta$ -diketo arm of **lg** interacts with IN amino acid residue ALA188 via hydrogen bond interaction. Clearly, the oxygens of the other triazolyl  $\beta$ -diketo arm of **lg** formed metal chelation with the two  $Mg^{2+}$  ions and interacts with IN amino acid residue GLU221 via hydrogen bond interaction. And the 1,2,3-triazole moiety interacts with PRO214 via C-H- $\pi$  and  $\pi$ - $\pi$  interactions.

In Fig 3c, the 4-methylphenyl group of one of the  $\beta$ -diketo arms of **4i** was accommodated at the hydrophobic cavity formed by IN amino acid residues ALA188, ALA189, PHE190, PRO161, and TYR129 with multiple C-H- $\pi$  and  $\pi$ - $\pi$  interactions, while raltegravir does not have any interactions in such hydrophobic cavity region [25]. Also, the 4-methylphenyl group of the other  $\beta$ -diketo arm of compound **4i** interacts with PRO214 and viral DNA via C-H- $\pi$  and  $\pi$ - $\pi$  interactions. Such interactions may result in that the  $\beta$ -diketo moiety or triazolyl  $\beta$ -diketo moiety are not coplane and lead to form partially metal chelation with the two  $Mg^{2+}$  ions.

The docking results reveal that the binding modes of these novel calix[4]arene derivatives **lg** and **4i** are different from the mechanism of action of the DKAs IN inhibitors raltegravir [5, 25]. The macrocyclic skeleton of calix[4]arene moiety of **lg** and **4i** may be fit for occupying the hydrophobic cavity and interact both with TYR212 and PRO214. While, raltegravir has no interaction with PRO214. One of the DKA pharmacophores

of **lg** and **4i** is just formed metal chelation partially with the two  $Mg^{2+}$  ions and do not interact with other amino acid residues in the docking simulation, which has a different binding behavior compared with the pyrimidone ring of raltegravir. And the other  $\beta$ -diketo arm of compound **4i** was accommodated at a new hydrophobic cavity, which no groups of raltegravir interact with it. Common integrase strand transfer inhibitors resistance pathways involve mutations of HIV-1 IN GLN148 or ASN155, which correspond to PFV IN residues SER217 and ASN224, respectively [25]. Obviously, the compounds **lg** and **4i** are predicted not to interact significantly with these key amino acids (GLN148 and ASN155) implicated in viral resistance in the docking studies [7, 8], which may be active toward IN strand transfer inhibitor resistant viral strains.

Clearly, the similar anti-IN activities between calix[4]arene derivatives **la-h** with triazolyl  $\beta$ -diketo arms and **4a-j** with  $\beta$ -diketo arms are very interesting, though these structures of **la-h** and **4a-j** are much more complicated than the structure of raltegravir. In the docking study, the binding modes of these novel calix[4]arene derivatives **lg** and **4i** are also similar to each other, but they have a different binding behavior distinguish with raltegravir. Based on the biological and virtual docking results, calix[4]arene derivatives incorporating two proper bi-substituted arms disposed in alternate positions at the lower rim maybe enhance the anti-IN activities.

## Conclusions

In summary, a series of calix[4]arene derivatives incorporating two  $\beta$ -diketo subunits disposed in alternate positions at the lower rim were synthesized and evaluated as HIV-1 integrase inhibitors. In general, compounds **4f-j** were active against the ST catalytic step, while the *tert*-butyl groups at the upper rim of calix[4]arene have a negative effect on inhibiting HIV-1 integrase ST reaction. Compared with the inhibition activities between our previous and current studies, the 1,2,3-triazole moiety maybe do not play an important role in the ST assay. Docking studies suggest that the macrocyclic skeletons of calix[4]arene moiety of the compounds **lg** and **4i** bind to the hydrophobic cavity in the IN active site. In particular, one of the  $\beta$ -diketo arms of compound **4i** dock into the hydrophobic cavity formed by IN amino acid residues, which is different from raltegravir binding behavior. Furthermore, no contacts with two of the most critical residues implicated in viral resistance, GLN148 and ASN155, were observed. This series of compounds could be further optimized to develop agents to overcome viral resistance against currently used HIV-1 IN inhibitors.

## Experimental

### Chemistry

Unless otherwise noted, all materials were obtained from commercial suppliers and dried and purified by standard

procedures. The melting point was measured on an SGW X-4 monocular microscope melting point apparatus with thermometer unadjusted.  $^1\text{H}$  NMR and  $^{13}\text{C}$  NMR spectra were acquired on a Bruker Avance III 400 MHz spectrometer with  $\text{CDCl}_3$  as the solvent and tetramethylsilane (TMS) as the internal standard. The chemical shifts were reported in  $\delta$  (ppm). Mass spectra (MS) data were obtained using Esquire 6000 mass spectrometer.

#### General methods for preparing compounds 4a–j

To a suspension of sodium hydride (60% dispersion in oil) (30 mmol) in dry THF (10 mL) was slowly added a range of acetophenones 3a–e (22 mmol) in dry THF (10 mL) at  $0^\circ\text{C}$  and the mixture was stirred for 10 min. After that, compound 2a or 2b (10 mmol) in dry THF (15 mL) was added to the above solution at  $0^\circ\text{C}$  and then the reaction mixture was slowly heated to refluxing for about 90 min with stirring till TLC confirmed that the reaction had finished. And then the cooled mixture was poured into a mixture of ice-water (20 mL) and concentrated HCl (5 mL), extracted with EtOAc and purified by flash chromatography on silica gel eluting with petroleum ether/ethyl acetate (15:1 to 8:1).

The  $^1\text{H}$  NMR,  $^{13}\text{C}$  NMR, and MS (ESI) spectra of 4a–j are provided online as Supporting Information.

#### 25,27-Bis[(Z)-4-phenyl-4-hydroxybut-3-en-2-one-1-methyl]-26,28-dihydroxy-5,11,17,23-tert-butylcalix[4]arene 4a

White powder, 58% yield; mp: 198–200°C;  $^1\text{H}$  NMR (400 MHz,  $\text{CDCl}_3$ )  $\delta$  0.95 (18H, s), 1.31 (18H, s), 3.42 (4H, d,  $J = 13.2$  Hz), 4.30 (4H, d,  $J = 13.2$  Hz), 4.55 (4H, s), 6.83 (4H, s), 7.13 (4H, s), 7.29 (2H, s), 7.35 (4H, t,  $J = 7.6$  Hz), 7.50 (2H, t,  $J = 7.6$  Hz), 7.58 (2H, s), 7.88 (4H, d,  $J = 7.6$  Hz), 15.34 (2H, s);  $^{13}\text{C}$  NMR (100 MHz,  $\text{CDCl}_3$ )  $\delta$  192.1, 183.3, 150.4, 148.9, 147.9, 142.3, 133.7, 132.7, 132.2, 128.1, 127.7, 127.6, 125.9, 125.2, 94.1, 34.0, 33.9, 31.7, 31.5, 30.9; ESI-MS ( $m/z$ ): 991.4 (M+Na) $^+$ .

#### 25,27-Bis[(Z)-4-(p-chlorophenyl)-4-hydroxybut-3-en-2-one-1-methyl]-26,28-dihydroxy-5,11,17,23-tert-butylcalix[4]arene 4b

White powder, 71% yield; mp: 188–190°C;  $^1\text{H}$  NMR (400 MHz,  $\text{CDCl}_3$ )  $\delta$  0.96 (18H, s), 1.33 (18H, s), 3.44 (4H, d,  $J = 13.2$  Hz), 4.30 (4H, d,  $J = 13.2$  Hz), 4.58 (4H, s), 6.85 (4H, s), 7.15 (4H, s), 7.22 (2H, s), 7.33 (4H, d,  $J = 8.4$  Hz), 7.55 (2H, s), 7.85 (4H, d,  $J = 8.4$  Hz), 15.33 (2H, s);  $^{13}\text{C}$  NMR (100 MHz,  $\text{CDCl}_3$ )  $\delta$  191.7, 182.4, 150.2, 148.7, 148.1, 142.6, 139.1, 132.3, 132.1, 128.9, 128.5, 127.7, 125.9, 125.3, 94.0, 34.1, 33.9, 31.7, 31.5, 30.9; ESI-MS ( $m/z$ ): 1035.5 (M–H) $^-$ .

#### 25,27-Bis[(Z)-4-(p-fluorophenyl)-4-hydroxybut-3-en-2-one-1-methyl]-26,28-dihydroxy-5,11,17,23-tert-butylcalix[4]arene 4c

Pink powder, 60% yield; mp: 202–204°C;  $^1\text{H}$  NMR (400 MHz,  $\text{CDCl}_3$ )  $\delta$  0.96 (18H, s), 1.32 (18H, s), 3.44 (4H, d,  $J = 13.2$  Hz), 4.31 (4H, d,  $J = 13.2$  Hz), 4.58 (4H, s), 6.86 (4H, s), 7.05 (4H, t,

$J = 8.4$  Hz), 7.15 (4H, s), 7.28 (2H, s), 7.56 (2H, s), 7.92–7.95 (4H, m), 15.43 (2H, s);  $^{13}\text{C}$  NMR (100 MHz,  $\text{CDCl}_3$ )  $\delta$  190.9, 183.0, 150.3, 148.8, 148.2, 142.6, 132.2, 130.2, 130.1, 127.7, 126.0, 125.4, 115.5, 115.3, 93.8, 34.1, 33.9, 31.7, 31.5, 30.9; ESI-MS ( $m/z$ ): 1003.6 (M–H) $^-$ .

#### 25,27-Bis[(Z)-4-(p-methylphenyl)-4-hydroxybut-3-en-2-one-1-methyl]-26,28-dihydroxy-5,11,17,23-tert-butylcalix[4]arene 4d

White powder, 43% yield; mp: 185–188°C;  $^1\text{H}$  NMR (400 MHz,  $\text{CDCl}_3$ )  $\delta$  0.94 (18H, s), 1.32 (18H, s), 2.42 (6H, s), 3.42 (4H, d,  $J = 13.2$  Hz), 4.33 (4H, d,  $J = 13.2$  Hz), 4.56 (4H, s), 6.83 (4H, s), 7.11–7.15 (8H, m), 7.19 (2H, s), 7.48 (2H, s), 7.75 (4H, d,  $J = 8.4$  Hz), 15.49 (2H, s);  $^{13}\text{C}$  NMR (100 MHz,  $\text{CDCl}_3$ )  $\delta$  191.1, 184.0, 150.4, 149.0, 148.0, 143.6, 142.3, 132.2, 131.2, 128.8, 127.8, 125.9, 125.3, 93.7, 34.0, 33.9, 31.7, 31.4, 30.9, 21.8; ESI-MS ( $m/z$ ): 995.7 (M–H) $^-$ .

#### 25,27-Bis[(Z)-4-(p-methoxyphenyl)-4-hydroxybut-3-en-2-one-1-methyl]-26,28-dihydroxy-5,11,17,23-tert-butylcalix[4]arene 4e

White powder, 61% yield; mp: 144–147°C;  $^1\text{H}$  NMR (400 MHz,  $\text{CDCl}_3$ )  $\delta$  0.94 (18H, s), 1.32 (18H, s), 3.43 (4H, d,  $J = 13.2$  Hz), 3.89 (6H, s), 4.33 (4H, d,  $J = 13.2$  Hz), 4.57 (4H, s), 6.80–6.82 (8H, m), 7.14 (4H, s), 7.20 (2H, s), 7.46 (2H, s), 7.83 (4H, d,  $J = 8.4$  Hz), 15.68 (2H, s);  $^{13}\text{C}$  NMR (100 MHz,  $\text{CDCl}_3$ )  $\delta$  189.8, 184.2, 163.4, 150.5, 148.9, 147.9, 142.3, 132.2, 129.8, 127.8, 126.5, 125.9, 125.3, 113.5, 93.3, 55.6, 34.0, 33.9, 31.7, 31.5, 30.9; ESI-MS ( $m/z$ ): 1027.5 (M–H) $^-$ .

#### 25,27-Bis[(Z)-4-phenyl-4-hydroxybut-3-en-2-one-1-methyl]-26,28-dihydroxy-calix[4]arene 4f

White powder, 58% yield; mp: 201–203°C;  $^1\text{H}$  NMR (400 MHz,  $\text{CDCl}_3$ )  $\delta$  3.51 (4H, d,  $J = 13.2$  Hz), 4.33 (4H, d,  $J = 13.2$  Hz), 4.52 (4H, s), 6.73–6.81 (4H, m), 6.94 (4H, d,  $J = 7.6$  Hz), 7.14 (4H, d,  $J = 7.6$  Hz), 7.39 (4H, t,  $J = 7.6$  Hz), 7.52 (2H, t,  $J = 7.2$  Hz), 7.63 (2H, s), 7.84 (2H, s), 7.93 (4H, d,  $J = 7.2$  Hz), 15.25 (2H, s);  $^{13}\text{C}$  NMR (100 MHz,  $\text{CDCl}_3$ )  $\delta$  191.6, 183.3, 152.9, 151.2, 134.0, 132.8, 132.6, 129.5, 128.9, 128.2, 127.8, 127.5, 126.3, 119.8, 94.2, 31.4; ESI-MS ( $m/z$ ): 767.1 (M+Na) $^+$ .

#### 25,27-Bis[(Z)-4-(p-chlorophenyl)-4-hydroxybut-3-en-2-one-1-methyl]-26,28-dihydroxy-calix[4]arene 4g

White powder, 62% yield; mp: 177–180°C;  $^1\text{H}$  NMR (400 MHz,  $\text{CDCl}_3$ )  $\delta$  3.53 (4H, d,  $J = 13.2$  Hz), 4.32 (4H, d,  $J = 13.2$  Hz), 4.56 (4H, s), 6.75–6.83 (4H, m), 6.95 (4H, d,  $J = 7.6$  Hz), 7.15 (4H, d,  $J = 7.6$  Hz), 7.36 (4H, d,  $J = 8.4$  Hz), 7.57 (2H, s), 7.76 (2H, s), 7.87 (4H, d,  $J = 8.4$  Hz), 15.24 (2H, s);  $^{13}\text{C}$  NMR (100 MHz,  $\text{CDCl}_3$ )  $\delta$  191.2, 182.5, 152.6, 151.0, 139.2, 132.7, 132.5, 129.6, 129.0, 128.8, 128.6, 127.8, 126.4, 120.0, 94.1, 31.4; ESI-MS ( $m/z$ ): 811.3 (M–H) $^-$ .

#### 25,27-Bis[(Z)-4-(p-fluorophenyl)-4-hydroxybut-3-en-2-one-1-methyl]-26,28-dihydroxy-calix[4]arene 4h

White powder, 66% yield; mp: 204–206°C;  $^1\text{H}$  NMR (400 MHz,  $\text{CDCl}_3$ )  $\delta$  3.52 (4H, d,  $J = 13.2$  Hz), 4.33 (4H, d,  $J = 13.2$  Hz),

4.55 (4H, s), 6.75–6.85 (4H, m), 6.96 (4H, d,  $J = 7.6$  Hz), 7.08 (4H, t,  $J = 8.4$  Hz), 7.15 (4H, d,  $J = 8.4$  Hz), 7.59 (2H, s), 7.81 (2H, s), 7.95–7.99 (4H, m), 15.33 (2H, s);  $^{13}\text{C}$  NMR (100 MHz,  $\text{CDCl}_3$ )  $\delta$  190.4, 183.1, 152.8, 151.0, 132.7, 130.5, 130.1, 129.6, 128.9, 127.8, 126.4, 120.0, 115.6, 115.4, 93.9, 31.4; ESI-MS ( $m/z$ ): 779.3 (M-H) $^-$ .

#### 25,27-Bis[(Z)-4-(p-methylphenyl)-4-hydroxybut-3-en-2-one-1-methyl]-26,28-dihydroxy-calix[4]arene **4i**

White powder, 48% yield; mp: 199–201°C;  $^1\text{H}$  NMR (400 MHz,  $\text{CDCl}_3$ )  $\delta$  2.43 (6H, s), 3.52 (4H, d,  $J = 13.2$  Hz), 4.35 (4H, d,  $J = 13.2$  Hz), 4.54 (4H, s), 6.74–6.83 (4H, m), 6.94 (4H, d,  $J = 7.6$  Hz), 7.14 (4H, d,  $J = 7.6$  Hz), 7.17 (4H, d,  $J = 8.4$  Hz), 7.51 (2H, s), 7.73 (2H, s), 7.78 (4H, d,  $J = 8.4$  Hz), 15.40 (2H, s);  $^{13}\text{C}$  NMR (100 MHz,  $\text{CDCl}_3$ )  $\delta$  190.7, 184.0, 153.1, 151.3, 143.7, 132.7, 131.3, 129.5, 129.0, 128.9, 127.8, 127.6, 126.2, 119.8, 93.8, 31.4, 21.8; ESI-MS ( $m/z$ ): 771.3 (M-H) $^-$ .

#### 25,27-Bis[(Z)-4-(p-methoxyphenyl)-4-hydroxybut-3-en-2-one-1-methyl]-26,28-dihydroxy-calix[4]arene **4j**

White powder, 42% yield; mp: 193–196°C;  $^1\text{H}$  NMR (400 MHz,  $\text{CDCl}_3$ )  $\delta$  3.52 (4H, d,  $J = 13.2$  Hz), 3.89 (6H, s), 4.36 (4H, d,  $J = 13.2$  Hz), 4.56 (4H, s), 6.75–6.81 (4H, m), 6.87 (4H, d,  $J = 8.4$  Hz), 6.94 (4H, d,  $J = 7.6$  Hz), 7.15 (4H, d,  $J = 7.6$  Hz), 7.49 (2H, s), 7.75 (2H, s), 7.88 (4H, d,  $J = 8.4$  Hz), 15.45 (2H, s);  $^{13}\text{C}$  NMR (100 MHz,  $\text{CDCl}_3$ )  $\delta$  189.4, 184.3, 163.5, 153.0, 151.3, 132.7, 129.8, 129.5, 128.9, 127.9, 126.7, 126.2, 119.8, 113.6, 93.3, 55.6, 31.4; ESI-MS ( $m/z$ ): 803.3 (M-H) $^-$ .

### HIV-1 integrase inhibitory assay

Compounds diluted in DMSO were pre-incubated with 800 ng integrase at 37.8°C in the reaction buffer in the absence of  $\text{Mg}^{2+}$  for 10 min. Subsequently, 1.5 pmol donor DNA and 9 pmol target DNA were added and the reaction was initiated by the addition of 10 mmol/L  $\text{Mg}^{2+}$  into the final reaction volume. The reactions were carried out at 37.8°C for 1 h and subsequent detection procedure was applied to detect the assay signals. Integrase inhibitor, raltegravir, was used as the control compound (positive control), and DMSO was set as the drug-free control (negative control). The inhibition effects of calix[4]arene-based  $\beta$ -diketo derivatives **4a–j** were calculated based on the positive and negative controls.

### Docking simulation

The receptor and all inhibitors were added Gasteiger charges, the box to a grid number was set to 60 (length)  $\times$  70 (wide)  $\times$  60 (high)  $\text{\AA}^3$  with a grid space of 0.375  $\text{\AA}$  in each dimension and the Lamarckian genetic algorithm was used for conformation search. A total of 100 docking conformations for echinomycin were generated and the maximum of evaluations set to  $2.5 \times 10^6$  to explore the conformational space, the remaining parameters take default values of AutoDock 4.2. The best binding conformation was selected for interaction analysis. The structure of inhibitors were drawn and refined by Discovery Studio 4.0. And all pictures

were generated by Discovery studio 4.0 (Accelrys Software, Inc., Discovery Studio Modeling Environment, Release 4.0, San Diego, CA).

The authors gratefully thank the financial supports of the Natural Science Foundation of China (Nos. 21102003, 21272020, 21102084, 81202438), Scientific Research Foundation for the Introduction of Talent of Anhui University of Science & Technology.

The authors have declared no conflict of interest.

### References

- [1] N. Vandegraaff, A. Engelman, *Expert Rev. Mol. Med.* **2007**, *9*, 1–19.
- [2] T. H. Evering, M. Markowitz, *Expert Opin. Invest. Drugs* **2008**, *17*, 413–422.
- [3] R. Dayam, R. Gundla, L. Q. Al-Mawsawi, N. Neamti, *Med. Res. Rev.* **2008**, *28*, 118–154.
- [4] J. A. Grobler, K. Stillmock, B. Hu, M. Witme, P. Felock, A. S. Espeseth, A. Wolfe, M. Egbertson, M. Bourgeois, J. Melamed, J. S. Wai, S. Young, J. Vacca, D. Hazuda, *J. Proc. Natl. Acad. Sci. USA* **2002**, *99*, 6661–6666.
- [5] A. Bacchi, M. Biemmi, M. Carcelli, C. Compari, E. Fiscaro, D. Rogolino, M. Sechi, M. Sippel, C. A. Sottriffer, T. W. Sanchez, N. Neamati, *J. Med. Chem.* **2008**, *51*, 7253–7264.
- [6] E. Serrao, S. Odde, K. Ramkumar, N. Neamati, *Retrovirology* **2009**, *6*, 25.
- [7] M. Metifiot, C. Marchand, K. Maddali, Y. Pommier, *Viruses* **2010**, *2*, 1347–1366.
- [8] M. A. Wainberg, T. Mesplede, P. K. Quashie, *Curr. Opin. Virol.* **2012**, *2*, 656–662.
- [9] C. Garrido, V. Soriano, A. M. Geretti, N. Zahonero, S. Garcia, C. Booth, F. Gutierrez, I. Viciano, C. deMendoza, *Antiviral Res.* **2011**, *90*, 164–167.
- [10] F. Christ, Z. Debyser, *Virology* **2013**, *435*, 102–109.
- [11] Z. G. Luo, X. M. Xu, X. M. Zhang, L. M. Hu, *Mini Rev. Med. Chem.* **2013**, *13*, 1160–1165.
- [12] De Fátima, S. A. Fernandes, A. A. Sabino, *Curr. Drug Discov. Tech.* **2009**, *6*, 151–170.
- [13] M. Mourer, N. Psychogios, G. Laumond, A. M. Aubertin, J. B. Regnouf-de-Vains, *Bioorg. Med. Chem.* **2010**, *18*, 36–45.
- [14] L. K. Tsou, G. E. Dutschman, E. A. Gullen, M. Telpoukhovskaia, Y. C. Cheng, A. D. Hamilton, *Bioorg. Med. Chem. Lett.* **2010**, *20*, 2137–2139.
- [15] Z. G. Luo, Y. Zhao, C. Ma, X. M. Xu, X. M. Zhang, N. Y. Huang, H. Q. He, *Chin. Chem. Lett.* **2014**, *25*, 737–740.
- [16] M. Yukito, H. Osamu, N. Yasuyuki, *J. Am. Chem. Soc.* **1994**, *116*, 2611–2612.
- [17] J. Guillon, J. M. Leger, P. Sonnet, C. Jarry, M. Robba, *J. Org. Chem.* **2000**, *65*, 8283–8289.

- [18] Z. G. Luo, Y. Zhao, C. Ma, L. Cao, S. H. Ai, J. S. Hu, X. M. Xu, *Chin. J. Struct. Chem.* **2014**, *33*, 1117–1122.
- [19] Z. G. Luo, C. Ma, L. M. Wu, M. H. Yuan, C. H. Xu, J. S. Hu, X. M. Xu, *Chin. J. Struct. Chem.* **2014**, *33*, 865–870.
- [20] V. S. Talanov, R. A. Bartsch, *J. Chem. Soc. Perkin Trans.* **1999**, *1*, 1957.
- [21] C. Jaime, J. De Mendoza, P. Prados, P. M. Nieto, C. Sanchez, *J. Org. Chem.* **1991**, *56*, 3372–3376.
- [22] J. Zawadiak, M. Mrzyczek, *Spectrochim. Acta. A Mol. Biomol. Spectrosc.* **2012**, *96*, 815–819.
- [23] H. Q. He, X. H. Ma, B. Liu, W. Z. Chen, C. X. Wang, S. H. Chen, *Acta Pharmacol. Sin.* **2008**, *29*, 397–404.
- [24] G. M. Morris, R. Huey, W. Lindstrom, M. F. Sanne, R. K. Belew, D. S. Goodsell, A. J. Olson, *J. Comput. Chem.* **2009**, *30*, 2785–2791.
- [25] S. Hare, S. S. Gupta, E. Valkov, A. Engelman, P. Cherepanov, *Nature* **2010**, *464*, 232–236.
- [26] S. H. Yu, T. W. Sanchez, Y. Liu, Y. Z. Yin, N. Neamati, G. S. Zhao, *Bioorg. Med. Chem. Lett.* **2013**, *23*, 6134–6137.